THE JOURNAL OF PHYSICAL CHEMISTRY B

Article

pubs.acs.org/JPCB

C−H···O Interaction in Methanol−Water Solution Revealed from Raman Spectroscopy and Theoretical Calculations

Yuanqin Yu,[†] Wei Fan,[‡] Yuxi Wang,[‡] Xiaoguo Zhou,[‡] Jin Sun,[†] and Shilin Liu*[,‡]

[†]Department of Physics, Anhui University, Hefei, Anhui, 230601, China

[‡]Hefei National Laboratory for Physical Sciences at the Microscale, iChEM (Collaborative Innovation Center of Chemistry for Energy Materials), Department of Chemical Physics, University of Science and Technology of China, Hefei 230026, China

Supporting Information

ABSTRACT: A combination of temperature-dependent Raman spectroscopy and quantum chemistry calculation was employed to investigate the blue shift of CH_3 stretching vibration in methanol−water mixtures. It shows that the conventional O−H···O hydrogen bonds do not fully dominate the origin of the C−H blue shift and the weak C−H···O interactions also contribute to it. This is consistent with the temperature-dependent results, which reveal that the C−H···O interaction is enhanced upon increasing the temperature, leading to further C−H blue shift in observed spectra at high temperature. This behavior is in contrast with the general trend that the conventional O−H···O hydrogen bond is destroyed by the temperature. The results will shed new light onto the nature of the C−H···O interaction and be helpful to understand hydrophilic and hydrophobic interactions of amphiphilic molecules in different environments.

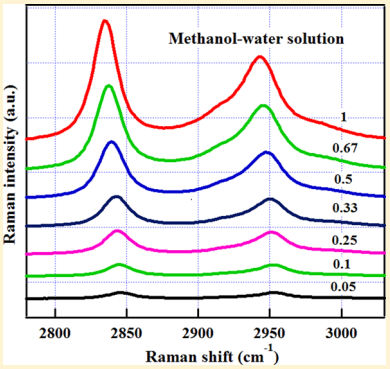

INTRODUCTION

Weak intermolecular forces determining the conformation of molecules and the molecular packing in crystals are currently the focus of extended studies. Hydrogen bond, the most common weak interaction in molecules, plays a fundamental role in physics, chemistry, biology, and material science.[1−4] Usually, the formation of the classic X−H···Y hydrogen bond leads to the X−H bond elongating with a concomitant red shift of its stretching frequency and an enhancement of the intensity in IR or Raman spectra, where X and Y are the electronegative atoms such as O, N, and F. The wavenumbers of red shift characterize the strength of the hydrogen bond. In recent years, much attention has been devoted to an unusual class of X−H···Y hydrogen bonds referred to as "improper blue-shifted" hydrogen bonds, where hydrogen is bonded to less electronegative atoms X, such as C, Si, and P.[5−15] It follows the opposite trend, a contraction of the X−H bond and a blue shift of stretching frequency with a reduced spectral intensity. A number of theoretical studies have been performed to explain the mechanism of blue shift. In Hobza et al.'s view,[10−12] the blue-shifted hydrogen bond behaves quite different from the red-shifted one. The formation of the conventional hydrogen bond is a direct process where the weakening of the X−H bond is caused by electron density transfer (EDT) from the proton acceptor to the antibond orbital of the proton donor, whereas the formation of the blue-shifted hydrogen bond is a more complicated "two-step" process where the strengthening of the X−H bond results from structural reorganization induced by EDT from the donor to a remote part of the acceptor, which in turn leads to a shortening of the X−H bond. On the basis of a thorough theoretical calculation, Scheiner et al. proposed that red-shifted and blue-shifted hydrogen bonds lead to a similar change in electron density of remote parts of the hydrogen bond donor and thus there are no fundamental distinctions between them.[13,14] The explanation on red-shifted and blue-shifted hydrogen bonds continues to be of interest nowadays.[16−24]

Among the blue-shifted X−H···Y hydrogen bonds, the C−H···O hydrogen bond is the most extensively studied both experimentally and theoretically. This is because the C−H group is ubiquitous in organic and biological molecules, and water is the most important solution. The accumulated evidence has shown that C−H···O interaction acts as an important factor in crystal packing, structure−activity relationship, and conformation stabilization of molecules and molecular assemblies in both chemistry and biochemistry.[7−9,25−29] For example, the C−H···O hydrogen bond contributing an additional stability to self-assembled β-sheet formation in 1-acetamido-3-(2-primidinnyl) imidazolium has been reported.[25] Recently, the strong C−H···O bifurcated interactions between the most acidic hydrogen atom of the cation imidazole ring and the oxygen atom of the anion were predicted in the room-temperature ionic liquid 1-ethyl-3-methylimidazolium trifluoromethanesulfonate using quantum chemical calculation.[27] However, compared to the conventional hydrogen bond, the C−H···O hydrogen bond is relatively weak, leading to the difficulty of obtaining conclusive experimental evidence. Nevertheless, the studies suggested that the strengths of the

Received: June 19, 2017
Revised: July 31, 2017
Published: August 9, 2017

DOI: 10.1021/acs.jpcb.7b06036
J. Phys. Chem. B 2017, 121, 8179−8187

C−H···O interaction can be enhanced in molecular aggregates containing charges or under the condition of high pressure.[25,30−32] In this work, we investigate the temperature-enhanced C−H···O interaction by choosing the methanol−water mixture as a model system.

Methanol is the simplest amphiphilic molecule containing both a hydrophilic group and a hydrophobic group. Therefore, a methanol and water mixture constitutes a model for investigation of the hydrophilic and hydrophobic effects in biological systems, since a good understanding of the hydration process of polar and nonpolar segments of methanol can help in the better understanding of aqueous solutions of more complex amphiphilic biomolecules which are difficult to study.[33−37] In addition, a methanol−water mixture itself exhibits many abnormal properties compared to pure liquid, which attract much interest in physics and chemistry.[38,39] For instance, the mixture of methanol and water exhibits an entropy value that is smaller than expected, which leads to the concept of negative excess entropy.[38] These intriguing properties are believed to be related to the hydration structures of methanol. Thus, understanding the origin of the anomalous behavior of the methanol−water system has been the subject of many studies.[40−47] The ice-like or clathrate-like structures created by the hydrophobic headgroups in the surrounding water was proposed to interpret it.[40−43] Also, a number of experimental and theoretical studies suggested that the methanol and water molecules cluster together with ring or chain forms.[36,44] On the basis of neutron diffraction measurements combined with the empirical potential structure refinement (EPSR) method, Dixit et al. suggested that the anomalous thermodynamics arises from incomplete mixing of methanol and water at the molecular level.[47] Further evidence of incomplete mixing has been presented by Guo et al., on the basis of X-ray emission spectroscopy.[45] More recently, Nagasaka et al. measured the C K-edge X-ray absorption spectra (XAS) of methanol−water solution $(CH_3OH)_X(H_2O)_{1-X}$.[48] They found that the hydrophobic interaction of the methyl group with water shows characteristic changes at the three concentration regions with the borders of molar fractions of methanol (X) equal to 0.7 and 0.3. With the help of molecular dynamics (MD) simulation, they proposed different local structures: in the methanol-rich region $X > 0.7$, a small amount of water molecules form the HB network with methanol clusters and the interaction around the methyl group of methanol is not so much influenced by isolated water molecules; in the region $0.7 > X > 0.3$, the hydrophobic interaction of the methyl group is dominant due to the increase of mixed methanol−water three-dimensional network structures; in the water-rich region $0.3 > X > 0.05$, methanol molecules are separately embedded in dominant three-dimensional hydrogen bond networks of water.

It is known that vibrational spectroscopy is a powerful method for the investigation of hydrogen bonding. Thus, the structure of liquid methanol−water solutions has also been extensively investigated by infrared and Raman spectroscopy in different spectral regions, including O−H stretching, C−H stretching, C−O stretching, and $-CH_3$ rocking regions.[49−56] For example, Dixit et al. measured high-resolution Raman spectra in C−O and C−H stretching regions by Raman spectroscopy.[51] They found a nonlinear dependence of both frequencies on the fraction of methanol in water solution and interpreted this in terms of a global picture of the progressive hydration of methanol. Interestingly, the C−H stretching spectrum of methanol was observed to be blue-shifted upon the dilution of water.[54−56] This is in agreement with the expected behavior for a blue-shifted C−H···O interaction formed between the O atom of water and the methyl group of methanol, as suggested by Keefe et. al.[55] In their studies, the C−H stretching spectra of methanol in different solvents, including water, acetonitrile, and carbon tetrachloride, were comparatively investigated in order to explore potential experimental evidence for C−H···O interaction. On the basis of IR spectral study on deuterated CH_2DOH in water, Shimoaka et al. attributed the C−D blue shift to the population change of the end-donor species in the hydrogen-bonding pattern.[56] In this study, Raman spectra of methanol−water mixtures were investigated in both C−H and O−H stretching regions by a combination of temperature-dependent Raman spectroscopy and quantum chemistry calculations, with the aim to shed light on the origin of the C−H blue shift and the nature of the C−H···O interaction that widely exists in organic and biological systems.

EXPERIMENTAL AND THEORETICAL METHODS

Methanol was purchased from Sigma-Aldrich. The water was triply distilled. All solutions were prepared by volume measurement of methanol and water to achieve the desired molar concentrations.

The Raman spectra of methanol in pure liquid state and in water solutions are recorded by conventional spontaneous Raman experiment. The instrument and setup parameters are similar to those reported previously.[53,57−60] Briefly, a cw laser (Coherent,Verdi-5W, 532 nm) was used as the light source with a power output of 4 W and the laser intensity at the sample was estimated to be 3.7×10^5 W/cm^2. During the experiments, the incident laser was linearly polarized with a Glan-laser prism, and its polarization direction was controlled vertically with a half-wave plate. The Raman scattering light was collected at 180° relative to the incident laser beam with a pair of f = 2.5 and 10 cm quartz lenses, and imaged onto the entrance slit of the monochromator (Acton Research, TriplePro) connected to a liquid-nitrogen-cooled CCD detector (Princeton Instruments, Spec-10:100B) to obtain experimental data. Between the two lenses, a Glan-Taylor prism and an optical scrambler were inserted. The Glan-Taylor prism was used to select the polarization of the scattering light which could be parallel and perpendicular to that of the excitation laser, and the scrambler was used to depolarize the polarized scattering light in order to eliminate any polarization-dependent effect from the dispersion gratings. In this experiment, only the Raman spectra with parallel polarizations were recorded. The 2400 groove/mm grating was used to record the C−H stretching spectrum with a spectral resolution of ∼1.0 cm^{-1}, while the 600 groove/mm grating was used to record the O−H stretching spectrum with a spectral resolution of ∼3.0 cm^{-1}. The precision of spectral measurement of both gratings was estimated to be better than 0.01 cm^{-1}. Each spectrum is an accumulation of 10 scans with a typical exposure time of 6 s.

For the measurements of temperature-dependent Raman spectra, a heating bath (THD-2006, Ningbo) was used to control the temperature (±0.1 °C) of the samples in a 10 × 10 mm^2 quartz cuvette.

All calculations were performed with the Gaussian 09 suite of programs,[61] including optimized structures, harmonic vibrational frequency, and binding energy of various hydrogen-bonded clusters formed between methanol and water molecules, using the MP2 method and 6-311++G(d,p) basis

DOI: 10.1021/acs.jpcb.7b06036
J. Phys. Chem. B 2017, 121, 8179−8187

sets, as has been successfully accomplished in studies of hydrogen-bonded complexes.[36] The calculated binding energies (ΔE) were corrected with basis set superposition errors (BSSE) using the counterpoise procedure (CP) suggested by Boys and Bernardi.[62] For a general methanol−(water)$_n$ cluster, the binding energy (ΔE) is defined as the following

$$\Delta E = E_{\text{cluster}} - (E_{\text{methanol}} + n^{*}E_{\text{water}}) + E_{\text{BSSE}} \quad (1)$$

where E_{cluster}, E_{methanol}, and E_{water} denote the electronic energies of methanol−(water)$_n$ cluster, methanol monomer, and water monomer corrected by zero-point vibrational energies (ZPE).

RESULTS AND DISCUSSION

C−H Stretching Spectra of Methanol in Aqueous Solution. Figure 1 presents concentration-dependent Raman spectra of methanol in the C−H stretching region from the pure liquid state to water solution with a molar fraction of methanol (X) at 0.67, 0.5, 0.33, 0.25, 0.1, and 0.05, respectively. In order to avoid the interference from the broad O−H band shape of water, the C−H spectrum was obtained by subtracting the pure water spectrum from the solution spectrum at each concentration, both of which were measured under the same experimental conditions. As seen from Figure 1, the methyl C−H stretching bands exhibit a systematic blue shift toward higher wavenumber as water concentrations increase. In previous studies, the vibrational spectrum of pure liquid methanol in the C−H stretching region has been well documented.[63−65] The most strong band at ∼2834 cm^{-1} was assigned to CH_3 symmetric stretching (CH_3-SS), the band at ∼2944 cm^{-1} and the shoulder at ∼2925 cm^{-1} were assigned to the Fermi resonance of the CH_3 bending overtone, and the weak shoulder at ∼2980 cm^{-1} was assigned to CH_3 antisymmetric stretching (CH_3-AS). Therefore, to determine the correct band center of C−H bands, the spectra at each concentration were fitted with four Lorentz functions. The frequency of the strong CH_3-SS band was chosen as the representative to plot versus the mole fractions of methanol in aqueous solution, as shown in Figure 2.

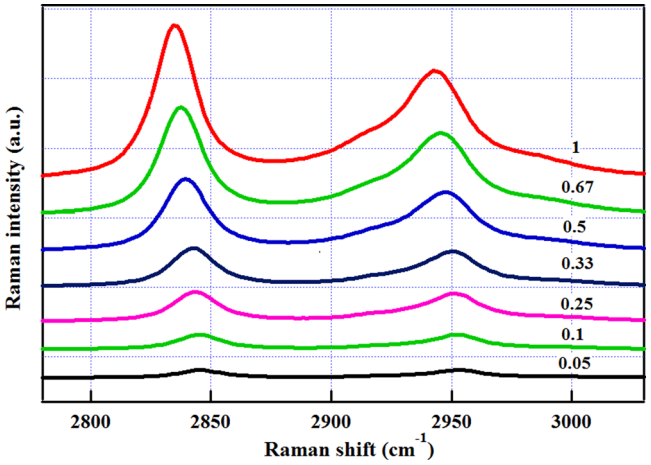

Figure 1. Concentration-dependent Raman spectra of methanol−water mixtures in the C−H stretching region with decreasing mole fraction of methanol from top to bottom.

It can be seen that the dependence of the CH_3-SS frequency on the mole fraction of methanol (X) clearly separates into three regions with different slopes. From X = 1 to X = 0.67, the CH_3-SS frequency increases gradually as the methanol concentration decreases. A much faster increase is noticed in the region from X = 0.67 to X = 0.33. The blue shift somewhat saturates at X = 0.33 but begins to increase again from X = 0.33 to X = 0.05. This observation is consistent with the measurement from Raman spectra in methanol−water solution by Dixit et al.,[51] in which a nonlinear dependence of both C−O and C−H stretching bands was observed in different concentrations with the borders of the fraction of methanol at X = 0.7 and X = 0.25. On the basis of the response of two kinds of spectra on concentrations, they propose a global picture of the progressive hydration of methanol: in the methanol-rich region, water molecules first connect the chain end of methanol molecules, and then, the chain structure of methanol is broken gradually by the water molecules in the concentration region from X = 0.7 to X = 0.25, and finally in the water-rich region, the process of hydration of methanol molecules is complete. In addition, in C K-edge XAS spectra of the methanol−water mixtures, similar nonlinear changes were also observed in three concentration regions with the borders at X = 0.7 and X = 0.3.[48] In this work, to further reveal the origin of the C−H blue shift in methanol−water solution, ab initio quantum chemistry calculations have been performed to examine the clusters formed between methanol and water molecules, with the aim to obtain the information on intermolecular interactions and the structure of clusters at the molecular level and to mimic the environment of methanol in the process of hydration.

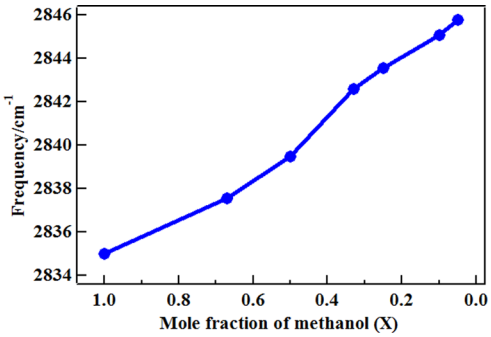

Figure 2. Concentration dependence of CH_3-SS frequency on the mole fraction of methanol in water solution.

Calculated Results. Figure 3 presents the optimized structures of methanol−(water)$_n$ clusters (MW$_n$, n = 1−4) and their isolated species calculated at the MP2/6-311++G(d,p) level. Table 1 summarizes the binding energy corrected with ZPE and BSSE, and the frequency of CH_3 symmetric stretching (CH_3-SS) along with blue shift relative to monomer methanol. The geometric parameters involved in C−H···O interaction are also listed. To contrast with the experimental spectra, a scale factor of 0.9512 was employed for the calculated harmonic vibrational frequency.[36,66]

From Figure 3, it can be seen that there are various kinds of hydrogen-bonded clusters formed between methanol and water molecules due to the amphiphilic nature of the methanol molecule. When n = 1, two heterodimers, MW$_1$-a and MW$_1$-b, are formed, in which the methanol molecule behaves as a proton acceptor and donor, respectively. In previous theoretical studies, there are some controversies regarding the relative stabilities of the structures MW$_1$-a and MW$_1$-b due to their small energy difference.[33,34] Our calculation at the MP2/6-311++G(d,p) level predicts that the MW$_1$-a is more stable than MW$_1$-b with a lower binding energy of about 0.3 kcal/mol,

DOI: 10.1021/acs.jpcb.7b06036
J. Phys. Chem. B 2017, 121, 8179−8187

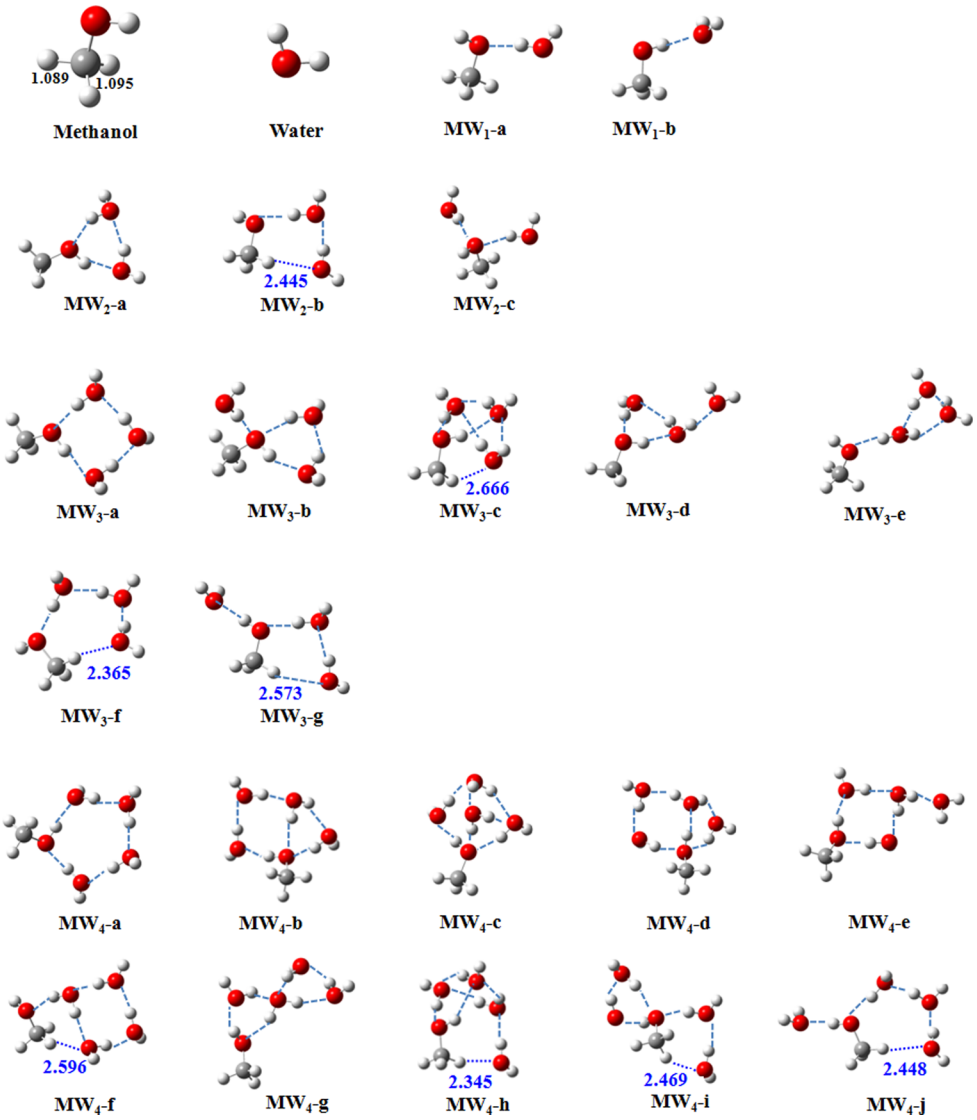

Figure 3. Optimized geometric structures of methanol−water clusters calculated at the MP2/6-311++g(d,p) level.

consistent with high-level theoretical calculation and gas-phase experiment under supersonic cooled molecular beam or in solid argon matrix.[33] As seen from Table 1, the calculated frequency of the CH_3-SS band in the MW_1-a structure is blue-shifted 16 cm^{-1} relative to monomer methanol, whereas, in MW_1-b, it is red-shifted 12 cm^{-1}. Therefore, the mean frequency of CH_3-SS is estimated to be blue-shifted at least 4 cm^{-1} when forming methanol−water dimers, according to the calculation.

For n = 2, three stable heterotrimers are obtained, as shown in Figure 3. The cyclic structure, MW_2-a, is the most stable with a binding energy of −8.82 kcal/mol. It consists of three O−H···O hydrogen bonds by all molecules being proton acceptor and proton donor at the same time, which indirectly lead to a 3 cm^{-1} blue shift in CH_3-SS frequency. The cyclic structure MW_2-b lies higher in energy than MW_2-a by 1.88 kcal/mol. For this structure, it can be seen that, in addition to the formation of conventional O−H···O hydrogen bonds, there is one C−H···O interaction simultaneously formed between the oxygen atom of the water molecule and one of the hydrogen atoms of the methyl group. To the best of our knowledge, there are no reports on the structure MW_2-b in a previous study. The geometric parameters for the C−H···O interaction of the MW_2-b structure are listed in Table 1. It can be seen that the distance of H···O is 2.445 Å and the angle of ∠CHO is 153.3°. According to the recent modern definition of hydrogen bonds proposed by Arunan et al.,[27,67] this C−H···O contact is accepted as a true hydrogen bond. It is much weaker than a covalent bond but stronger than van der Waals (VDW) interactions. With this C−H···O interaction, the in-plane C−H bond in the MW_2-b structure is shortened by 0.0012 Å compared to that in monomer methanol, leading to a 15 cm^{-1} blue shift on the CH_3-SS band, where the plane denotes H−C−O−H in the methanol molecule. The third heterotrimer MW_2-c is a chain-like structure with the highest binding energy of −5.09 kcal/mol, formed via two O−H···O hydrogen bonds. The blue shift in this structure is as large as 30 cm^{-1}. From the above calculations, it is clear that the formation of all three heterotrimers MW_2 results in the C−H blue shift in an indirect or direct way.

For n = 3, seven stable structures are optimized. Among them, the four structures, MW_3-a, MW_3-b, MW_3-d, and MW_3-e, are totally formed via O−H···O hydrogen bonds, while three structures, MW_3-c, MW_3-f, and MW_3-g, are participating in both O−H···O and C−H···O hydrogen bonds. The cyclic

DOI: 10.1021/acs.jpcb.7b06036
J. Phys. Chem. B 2017, 121, 8179−8187

Table 1. Calculated CH_3-SS Stretching Frequency (cm^{-1}) and Binding Energies ΔE (in kcal/mol) of Methanol−$(Water)_n$ Clusters (MW_n, n = 1−4) along the Geometric Parameters Involved in C−H···O Interaction

							parameters of C−H···O interaction		
n	complex	$\upsilon_{CH_3\text{-}SS}$ [a]	$\Delta\upsilon_{CH_3\text{-}SS}$ [b]	E_{ZPE} [c]	E_{BSSE} [d]	$\Delta E_{BSSE+ZPE}$ [e]	R(H···O) (Å)	∠CHO	R(C−H) [f] (Å)
0	methanol	2905		32.74					1.0898 (in), 1.0958 (out)
1	MW_1-a	2921	16	48.45	1.78	−2.78			
	MW_1-b	2893	−12	48.19	1.82	−2.48			
2	MW_2-a	2908	3	64.91	4.28	−8.82			
	MW_2-b	2921	15	64.60	4.11	−6.91	2.445	153.3°	1.0886 (in)
	MW_2-c	2935	30	63.51	3.12	−5.09			
3	MW_3-a	2911	6	81.60	8.10	−15.80			
	MW_3-b	2920	15	80.33	6.28	−11.75			
	MW_3-c	2921	16	80.94	6.77	−11.62	2.666	132.8°	1.0932 (out)
	MW_3-d	2903	−2	80.31	6.07	−11.28			
	MW_3-e	2921	16	80.78	6.10	−11.06			
	MW_3-f	2921	16	80.68	6.74	−10.96	2.365	166.3°	1.0885 (in)
	MW_3-g	2914	9	80.02	6.27	−10.33	2.573	148.2°	1.0896 (out)
4	MW_4-a	2911	6	97.61	11.01	−20.86			
	MW_4-b	2914	9	97.45	10.30	−20.07			
	MW_4-c	2916	11	97.39	10.24	−19.40			
	MW_4-d	2913	8	97.36	9.97	−18.90			
	MW_4-e	2909	4	97.00	9.91	−18.15			
	MW_4-f	2917	12	97.58	10.21	−17.91	2.596	156.3°	1.0893 (in)
	MW_4-g	2910	5	97.24	8.78	−17.12			
	MW_4-h	2926	21	97.03	9.13	−16.09	2.345	163.6°	1.0917 (out)
	MW_4-i	2925	20	96.57	8.88	−15.39	2.469	141.3°	1.0920 (out)
	MW_4-j	2914	9	96.09	8.94	−14.38	2.448	161.6°	1.0892 (in)

[a]Scaled by a factor of 0.9512. [b]The frequency shift of CH_3-SS relative to monomer methanol. [c]The energy of zero point correction in kcal/mol. [d]Energy of BSSE correction in kcal/mol. [e]Binding energy corrected by ZPE and BSSE. [f]C−H bond length of methanol, and the "in" or "out" in brackets denote the C−H bond in the plane and out of the plane, where the plane is H−C−O−H in the methanol molecule.

structure MW_3-a is still the most stable with a binding energy of −15.8 kcal/mol, which is lower by 3.95−4.83 kcal/mol than all other clusters. Similar to the MW_2 clusters, the formation of MW_3 clusters leads to the blue shift of the CH_3-SS band except for the MW_3-e structure, in which the red shift occurs, as summarized in Table 1. It is interesting to find that, with C−H···O interaction, a three-dimensional cage-like feature appears in the MW_3-c structure, whereas all other clusters present two-dimensional features with ring or chain forms.

For n = 4, 10 stable methanol−$(water)_4$ clusters are obtained, and four structures, MW_4-f, MW_4-h, MW_4-i, and MW_4-j, are involved in a weak C−H···O hydrogen bond. With the increase of cluster size, more clusters present three-dimensional features such as the MW_4-c and MW_4-h. This result is consistent with the previous molecular dynamical simulation, in which the one-dimensional chain structure of methanol molecules is changed to three-dimensional mixed clusters by adding water molecules.[68] Among all of the methanol−$(water)_4$ clusters, the cyclic MW_4-a structure is still the most stable with a binding energy of −20.8 kcal/mol and the calculated CH_3-SS bands in all clusters show blue shifts relative to monomer methanol, as listed in Table 1. Additionally, comparing the geometry parameters of those clusters involved in C−H···O interaction, it is clear that, with an increase in the number of water molecules, the C−H···O interaction is strengthened. For instance, in the MW_2-b structure, the distance of R(O···H) is 2.445 Å, whereas, in MW_3-c and MW_4-h, this distance becomes 2.365 and 2.345 Å, shortened by 0.08 and 0.1 Å, respectively.

Since the number of methanol−$(water)_n$ clusters increases exponentially with the increase of n, we do not perform the calculation on clusters of n larger than 4. However, from the above calculations on methanol−$(water)_n$ (n = 1−4) clusters, it can be seen that the conventional O−H···O hydrogen bond and weak C−H···O hydrogen bond coexist in the methanol−water mixture and both types of hydrogen bonds lead to a C−H blue shift. On the other hand, as shown in Table 1, the calculated blue shift presents a positive correlation with the addition of a water molecule. This is consistent with experimental observation (Figure 1), where the CH_3-SS frequency of methanol shifts to higher wavenumbers with the increase of water concentration. Therefore, the calculated results quantitatively support experimental observations. The further analysis on the calculated MW_n clusters also shows that the most obvious C−H blue shift occurs at n = 2, since the blue shifts in MW_2-a, MW_2-b, and MW_2-c are 3, 15, and 30 cm^{-1}, respectively, which are relatively larger than those in other clusters, in good agreement with the behavior of the steeper slope of the line of the concentration-dependent methanol−water mixture at a mole fraction of methanol equal to 0.33, as presented in Figure 2.

It should be noted that, according to the calculations, the binding energies of clusters that are totally connected via O−H···O hydrogen bonds are much lower than those clusters involved in C−H···O interaction for each kind of MW_n cluster, as listed in Table 1. In this way, it seems that the blue shift of the CH_3-SS band is overwhelming caused by the indirect effect of the O−H···O hydrogen bond according to the calculation. Although a large amount of literature suggested that the methanol and water molecules form hydrogen-bond rings or chains in the mixture, the calculated cluster presented here is based on the gas-phase structures free from the intermolecular interactions and thus cannot completely mimic real environ-

DOI: 10.1021/acs.jpcb.7b06036
J. Phys. Chem. B 2017, 121, 8179−8187

ments in the condensed phase. This will result in the difference between the calculated structures and observed ones in liquid methanol−water solution, such as the energy and the preferential conformations of clusters. In order to check the contribution of C−H···O interaction to the methyl blue shift, the temperature-dependent Raman spectra are conducted for methanol−water mixtures in both C−H and O−H stretching regions.

Temperature-Dependent Raman Spectra. Figure 4 displays temperature-dependent C−H stretching Raman spectra of methanol−water mixtures at a mole fraction of methanol equal to 0.1 measured at 5, 40, and 75°, respectively (the spectra at a mole fraction of methanol equal to 0.25 are listed in the Supporting Information, Figure S1). It can be seen that the band at 2834 cm^{-1} is slightly blue-shifted as the temperature goes up. Although this blue shift is subtle (about 1.2 cm^{-1}), it can still be observed. To contrast with the C−H spectra, the dependence of the O−H stretching spectra on temperature is also measured in the same concentration and temperature ranges, as presented in Figure 5, where only the spectra at temperatures of 5 and 75° were shown in order to be clear. It can be seen that the O−H spectra exhibit an obvious blue shift from 5 to 75°. Two main bands centered at ∼3190 and 3389 cm^{-1} are shifted to about 3221 and 3415 cm^{-1}, and the intensity of the former decreases, whereas the latter increases, suggesting that the large size methanol−water clusters are transferred to small size ones due to the destruction of O−H···O hydrogen bonds at high temperature. This means that the O−H blue shift at high temperature is a direct consequence of breaking of a conventional hydrogen bond, since the formation of the O−H···O hydrogen bond causes a red shift in a normal case. However, for the blue-shifted C−H spectra at high temperature, the mechanism should be different.

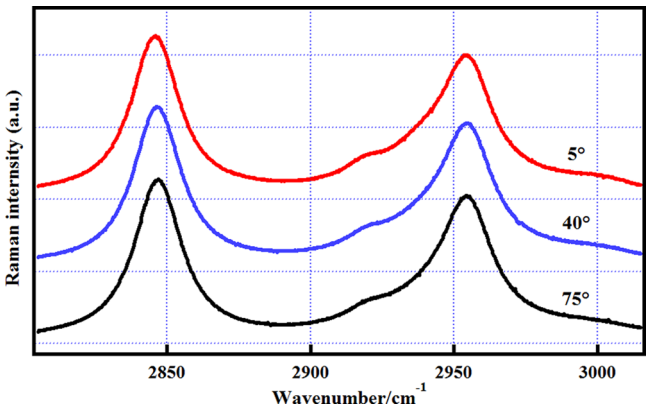

Figure 4. Temperature-dependent C−H stretching Raman spectra of the methanol−water mixture at a mole fraction of methanol equal to 0.1.

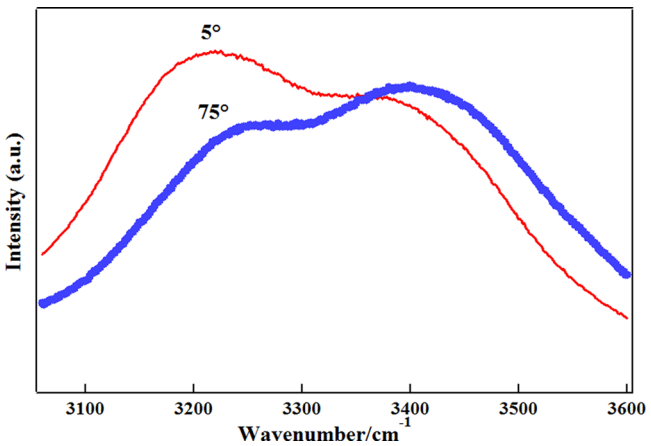

Figure 5. Temperature-dependent O−H stretching Raman spectra of the methanol−water mixture at a mole fraction of methanol equal to 0.1.

As illustrated by theoretical calculations in Table 1, the CH_3 stretching frequency of methanol is blue-shifted with the addition of water molecules, and this blue shift may arise from two origins. One is the indirect effect induced by the O−H···O hydrogen bond and the other is the direct C−H···O interaction from the H atom of the methyl group and O atom of the water molecule. If the blue shift of C−H spectra observed in Figure 1 is from O−H···O hydrogen bond interaction, the C−H spectra should be red-shifted at high temperature due to the destruction of the O−H···O hydrogen bond. However, this is obviously not true in experiment, since the C−H spectra of methanol are observed to be blue-shifted as the temperature is rising. Therefore, we conclude that the C−H blue shift in methanol−water solution should be from another origin, C−H···O interaction.

On the other hand, as seen from Table 1, the calculated C−H blue shift presents a positive correlation with the addition of water molecules. Although the large size methanol−water mixed clusters are transferred to small size ones due to the destruction of the O−H··· O hydrogen bond at high temperature, this should not cause the blue shift of the C−H spectra. Therefore, the C−H blue shift at high temperature should be from the increase of C−H···O interaction. A similar enhanced effect was also observed by the Chang group under high pressure conditions in the solutions.[25,30−32] In their studies, the conventional O−H···O hydrogen bond was also destroyed by high pressure, while the C−H···O interaction was enhanced. As mentioned earlier, the conclusive experimental evidence for C−H···O interaction is very difficult to obtain, since it is weak and usually coexists with the conventional hydrogen bond. Here, on the basis of the spectral response to temperature, we provide clear experimental evidence that C−H···O interaction exists in methanol−water solution and plays a role in the determination of the C−H blue shift.

The enhanced-temperature effect of C−H···O interaction is easy to be understood when considering many contrary behaviors between red-shifted and blue-shifted hydrogen bonds, such as different ways in bond length change and frequency shift. A similar result was obtained in a theoretical study on the cooperativity between O−H···O and C−H···O hydrogen bonds of a DMSO−H_2O complex.[69,70] It was shown that both types of interactions are changed differently when the cooperativity happens. The O−H···O hydrogen bond is weakened, whereas the C−H···O hydrogen bond is enhanced. As mentioned above, the enhanced effect of C−H···O interaction was also shown by the Chang group in a series of high-pressure studies.[25,30−32] These results imply that properties of the C−H···O hydrogen bond may behave differently from those of the conventional hydrogen bond in many aspects.

CONCLUSION

In this paper, we investigated the origin of the blue shift of CH_3 stretching vibration in methanol−water mixtures by temper-

DOI: 10.1021/acs.jpcb.7b06036
J. Phys. Chem. B 2017, 121, 8179−8187

ature-dependent Raman spectroscopy and quantum chemistry calculation. On the basis of the spectral response to temperature and the calculated structures for methanol−$(water)_n$ (n = 1−4) clusters, we provide clear experimental evidence that the weak C−H···O hydrogen bond coexists with a conventional O−H···O hydrogen bond in methanol−water solution and plays a role in the determination of C−H blue shift. Moreover, the comparative study of temperature-dependent spectra in both C−H and O−H stretching regions shows that the C−H···O interaction behaves differently from a conventional O−H···O hydrogen bond upon the temperature increasing. The former is enhanced, whereas the latter is weakened. As hydrogen bonding interactions are the most important noncovalent interactions in chemical and biological systems, our results presented here will be helpful to understand hydrophobic hydration mechanisms of biological systems in different chemical environments.

■ ASSOCIATED CONTENT

Supporting Information

The Supporting Information is available free of charge on the ACS Publications website at DOI: 10.1021/acs.jpcb.7b06036.

Temperature-dependent C−H stretching Raman spectra of a methanol−water mixture at a mole fraction of methanol equal to 0.25 (PDF)

■ AUTHOR INFORMATION

Corresponding Author

*E-mail: slliu@ustc.edu.cn.

ORCID

Yuanqin Yu: 0000-0001-7647-8404

Xiaoguo Zhou: 0000-0002-0264-0146

Notes

The authors declare no competing financial interest.

■ ACKNOWLEDGMENTS

The present work was supported financially by the National Natural Science Foundation of China (NSFC, 20903002, 21573208, 21573210), Anhui Provincial Educational Ministry (KJ2015A040), and National Key Basic Research Special Foundation (NKBRSF, 2013CB834602).

■ REFERENCES

(1) Jeffrey, G. A.; Saenger, W. *Hydrogen Bonding in Biological Structures*; Springer-Verlag: Berlin, 1991.

(2) Desiraju, G. R.; Steiner, T. *The Weak Hydrogen Bonding in Structural Chemistry and Biology*; Oxford University Press: Oxford, NY, 1999.

(3) Singh, P. C.; Inoue, K.; Nihonyanagi, S.; Yamaguchi, S.; Tahara, T. Femtosecond hydrogen bond dynamics of bulk-like and bound water at positively and negatively charged lipid interfaces revealed by 2D HD-VSFG spectroscopy. *Angew. Chem., Int. Ed.* **2016**, *55*, 10621−10625.

(4) Bakker, D. J.; Peters, A.; Yatsyna, V.; Zhaunerchyk, V.; Rijs, A. M. Far-infrared signatures of hydrogen bonding in phenol derivatives. *J. Phys. Chem. Lett.* **2016**, *7*, 1238−1243.

(5) Desiraju, G. R. The C-H···O hydrogen-bond in crystals - what is it. *Acc. Chem. Res.* **1991**, *24*, 290−296.

(6) Zierkiewicz, W.; Michalska, D.; Havlas, Z.; Hobza, P. Study of the nature of improper blue-shifting hydrogen bonding and standard hydrogen bonding in the X3CH center dot center dot center dot OH2 and XH center dot center dot center dot OH2 complexes (X = F, Cl, Br, I): A correlated ab initio study. *ChemPhysChem* **2002**, *3*, 511−518.

(7) Vaz, P. D.; Ribeiro-Claro, P. J. A. C-H center dot center dot center dot O hydrogen bonds in liquid cyclohexanone revealed by the vC═O splitting and the vC-H blue shift. *J. Raman Spectrosc.* **2003**, *34*, 863−867.

(8) Nolasco, M. M.; Ribeiro-Claro, P. J. A. C-H center dot center dot center dot O hydrogen bonds in cyclohexenone reveal the spectroscopic behavior of C-sp3-H and C-sp2-H donors. *ChemPhysChem* **2005**, *6*, 496−502.

(9) Scheiner, S. Identification of spectroscopic patterns of CH center dot center dot center dot O H-bonds in proteins. *J. Phys. Chem. B* **2009**, *113*, 10421−10427.

(10) Reimann, B.; Buchhold, K.; Vaupel, S.; Brutschy, B.; Havlas, Z.; Spirko, V.; Hobza, P. Improper, blue-shifting hydrogen bond between fluorobenzene and fluorobenzene. *J. Phys. Chem. A* **2001**, *105*, 5560−5566.

(11) van der Veken, B. J.; Herrebout, W. A.; Szostak, R.; Shchepkin, D. N.; Havlas, Z.; Hobza, P. The nature of improper, blue-shifting hydrogen bonding verified experimentally. *J. Am. Chem. Soc.* **2001**, *123*, 12290−12293.

(12) Hobza, P.; Havlas, Z. Improper, blue-shifting hydrogen bond. *Theor. Chem. Acc.* **2002**, *108*, 325−334.

(13) Gu, Y. L.; Kar, T.; Scheiner, S. Fundamental properties of the CH center dot center dot center dot O interaction: Is it a true hydrogen bond? *J. Am. Chem. Soc.* **1999**, *121*, 9411−9422.

(14) Scheiner, S.; Kar, T. Red- versus blue-shifting hydrogen bonds: Are there fundamental distinctions? *J. Phys. Chem. A* **2002**, *106*, 1784−1789.

(15) Hauchecorne, D.; Nagels, N.; van der Veken, B. J.; Herrebout, W. A. C-X center dot center dot center dot pi halogen and C-H center dot center dot center dot pi hydrogen bonding: interactions of CF3X (X = Cl, Br, I or H) with ethene and propene. *Phys. Chem. Chem. Phys.* **2012**, *14*, 681−690.

(16) Masunov, A.; Dannenberg, J. J.; Contreras, R. H. C-H bond-shortening upon hydrogen bond formation: Influence of an electric field. *J. Phys. Chem. A* **2001**, *105*, 4737−4740.

(17) Hermansson, K. Blue-shifting hydrogen bonds. *J. Phys. Chem. A* **2002**, *106*, 4695−4702.

(18) Li, X. S.; Liu, L.; Schlegel, H. B. On the physical origin of blue-shifted hydrogen bonds. *J. Am. Chem. Soc.* **2002**, *124*, 9639−9647.

(19) Alabugin, I. V.; Manoharan, M.; Peabody, S.; Weinhold, F. Electronic basis of improper hydrogen bonding: A subtle balance of hyperconjugation and rehybridization. *J. Am. Chem. Soc.* **2003**, *125*, 5973−5987.

(20) Barnes, A. J. Blue-shifting hydrogen bonds - are they improper or proper? *J. Mol. Struct.* **2004**, *704*, 3−9.

(21) Chang, X.; Zhang, Y.; Weng, X. Z.; Su, P. F.; Wu, W.; Mo, Y. R. Red-shifting versus blue-shifting hydrogen bonds: perspective from Ab Initio valence bond theory. *J. Phys. Chem. A* **2016**, *120*, 2749−2756.

(22) Wang, C. W.; Danovich, D.; Shaik, S.; Mo, Y. R. A unified theory for the blue- and red-shifting phenomena in hydrogen and halogen bonds. *J. Chem. Theory Comput.* **2017**, *13*, 1626−1637.

(23) Inagaki, S.; Murai, H.; Takeuchi, T. Theory of electron localization and its application to blue-shifting hydrogen bonds. *Phys. Chem. Chem. Phys.* **2012**, *14*, 2008−2014.

(24) Karpfen, A. Blue-shifted A-H stretching frequencies in complexes with methanol: the decisive role of intramolecular coupling. *Phys. Chem. Chem. Phys.* **2011**, *13*, 14194−14201.

(25) Lee, K. M.; Chang, H. C.; Jiang, J. C.; Chen, J. C. C.; Kao, H. E.; Lin, S. H.; Lin, I. J. B. C-H—O hydrogen bonds in beta-sheetlike networks: Combined X-ray crystallography and high-pressure infrared study. *J. Am. Chem. Soc.* **2003**, *125*, 12358−12364.

(26) Matsuura, H.; Yoshida, H.; Hieda, M.; Yamanaka, S.; Harada, T.; Shin-ya, K.; Ohno, K. Experimental evidence for intramolecular blue-shifting C-H···O hydrogen bonding by matrix-isolation infrared spectroscopy. *J. Am. Chem. Soc.* **2003**, *125*, 13910−13911.

(27) Singh, D. K.; Rathke, B.; Kiefer, J.; Materny, A. Molecular structure and Iinteractions in the ionic liquid 1-Ethyl-3-methylimidazolium trifluoromethanesulfonate. *J. Phys. Chem. A* **2016**, *120*, 6274−6286.

DOI: 10.1021/acs.jpcb.7b06036
J. Phys. Chem. B 2017, 121, 8179−8187

(28) Lavanya, P.; Ramaiah, S.; Anbarasu, A. Influence of C-H···O interactions on the structural stability of beta-lactamases. *J. Biol. Phys.* **2013**, *39*, 649−663.
(29) Jiang, J. C.; Li, S. C.; Shih, P. M.; Hung, T. C.; Chang, S. C.; Lin, S. H.; Chang, H. C. A high-pressure infrared spectroscopic study on the interaction of ionic liquids with PEO-PPO-PEO block copolymers and 1,4-dioxane. *J. Phys. Chem. B* **2011**, *115*, 883−888.
(30) Chang, H. C.; Jiang, J. C.; Chuang, C. W.; Lin, S. H. Evidence for hydrogen bond-like C-H-O interactions in aqueous 1,4-dioxane probed by high pressure. *Chem. Phys. Lett.* **2004**, *397*, 205−210.
(31) Chang, H. C.; Jiang, J. C.; Su, C. C.; Lu, L. C.; Hsiao, C. J.; Chuang, C. W.; Lin, S. H. Pressure-enhanced C-H center dot center dot center dot O interactions in aqueous tert-butyl alcohol. *J. Phys. Chem. A* **2004**, *108*, 11001−11005.
(32) Lee, K. M.; Chang, H. C.; Jiang, J. C.; Lu, L. C.; Hsiao, C. J.; Lee, Y. T.; Lin, S. H.; Lin, I. J. B. Probing C-H center dot center dot center dot X hydrogen bonds in amide-functionalized imidazolium salts under high pressure. *J. Chem. Phys.* **2004**, *120*, 8645−8650.
(33) González, L.; Mó, O.; Yáneza, M. High level ab initio and density functional theory studies on methanol−water dimers and cyclic methanol(water)2 trimer. *J. Chem. Phys.* **1998**, *109*, 139−150.
(34) Fileti, E. E.; Canuto, S. Calculated infrared spectra of hydrogen-bonded methanol-water, water-methanol, and methanol-methanol complexes. *Int. J. Quantum Chem.* **2005**, *104*, 808−815.
(35) Ruckenstein, E.; Shulgin, I. L.; Tilson, J. L. Treatment of dilute clusters of methanol and water by a initio quantum mechanical calculations. *J. Phys. Chem. A* **2005**, *109*, 807−815.
(36) Mandal, A.; Prakash, M.; Kumar, R. M.; Parthasarathi, R.; Subramanian, V. Ab initio and DFT studies on methanol-water clusters. *J. Phys. Chem. A* **2010**, *114*, 2250−2258.
(37) Deng, G. H.; Shen, Y. N.; He, Z. G.; Zhang, Q.; Jiang, B.; Yuan, K. J.; Wu, G. R.; Yang, X. M. The molecular rotational motion of liquid ethanol studied by ultrafast time resolved infrared spectroscopy. *Phys. Chem. Chem. Phys.* **2017**, *19*, 4345−4351.
(38) Lama, R. F.; Lu, B. C. Y. Excess thermodynamic properties of aqueous alcohol solutions. *J. Chem. Eng. Data* **1965**, *10*, 216−219.
(39) Benson, G. C.; Darcy, P. J. Excess isobaric hear-capacities of water normal-alcohol mixtures. *J. Chem. Eng. Data* **1982**, *27*, 439−442.
(40) Frank, H. S.; Evans, M. W. Free volume and entropy in condensed systems. III. Entropy in binary liquid mixtures; partial molal entropy in dilute solutions; structure and thermodynamics in aqueous electrolytes. *J. Chem. Phys.* **1945**, *13*, 507−532.
(41) Dolenko, T. A.; Burikov, S. A.; Dolenko, S. A.; Efitorov, A. O.; Plastinin, I. V.; Yuzhakov, V. I.; Patsaeva, S. V. Raman spectroscopy of water-ethanol solutions: The estimation of hydrogen bonding energy and the appearance of clathrate-like structures in solutions. *J. Phys. Chem. A* **2015**, *119*, 10806−10815.
(42) Holden, C. A.; Hunnicutt, S. S.; Sanchez-Ponce, R.; Craig, J. M.; Rutan, S. C. Study of complexation in methanol/water mixtures by infrared and Raman spectroscopy and multivariate curve resolution - alternating least-squares analysis. *Appl. Spectrosc.* **2003**, *57*, 483−490.
(43) Gong, Y. Y.; Xu, Y.; Zhou, Y.; Li, C.; Liu, X. J.; Niu, L. Y.; Huang, Y. L.; Zhang, X.; Sun, C. Q. Hydrogen bond network relaxation resolved by alcohol hydration (methanol, ethanol, and glycerol). *J. Raman Spectrosc.* **2017**, *48*, 393−398.
(44) Corsaro, C.; Spooren, J.; Branca, C.; Leone, N.; Broccio, M.; Kim, C.; Chen, S. H.; Stanley, H. E.; Mallamace, F. Clustering dynamics in water/methanol mixtures: A nuclear magnetic resonance study at 205 K < T < 295 K. *J. Phys. Chem. B* **2008**, *112*, 10449−10454.
(45) Guo, J. H.; Luo, Y.; Augustsson, A.; Kashtanov, S.; Rubensson, J. E.; Shuh, D. K.; Agren, H.; Nordgren, J. Molecular structure of alcohol-water mixtures. *Phys. Rev. Lett.* **2003**, *91*, 157401.
(46) Allison, S. K.; Fox, J. P.; Hargreaves, R.; Bates, S. P. Clustering and microimmiscibility in alcohol-water mixtures: Evidence from molecular-dynamics simulations. *Phys. Rev. B: Condens. Matter Mater. Phys.* **2005**, *71*, 024201.
(47) Dixit, S.; Crain, J.; Poon, W. C. K.; Finney, J. L.; Soper, A. K. Molecular segregation observed in a concentrated alcohol-water solution. *Nature* **2002**, *416*, 829−832.
(48) Nagasaka, M.; Mochizuki, K.; Leloup, V.; Kosugi, N. Local structures of methanol-water binary solutions studied by soft X-ray absorption spectroscopy. *J. Phys. Chem. B* **2014**, *118*, 4388−4396.
(49) Ebukuro, T.; Takami, A.; Oshima, Y.; Koda, S. Raman spectroscopic studies on hydrogen bonding in methanol and methanol/water mixtures under high temperature and pressure. *J. Supercrit. Fluids* **1999**, *15*, 73−78.
(50) Gruenloh, C. J.; Florio, G. M.; Carney, J. R.; Hagemeister, F. C.; Zwier, T. S. C-H stretch modes as a probe of H-bonding in methanol-containing clusters. *J. Phys. Chem. A* **1999**, *103*, 496−502.
(51) Dixit, S.; Poon, W. C. K.; Crain, J. Hydration of methanol in aqueous solutions: a Raman spectroscopic study. *J. Phys.: Condens. Matter* **2000**, *12*, L323−L328.
(52) Del Corro, E.; Caceres, M.; Taravillo, M.; Nunez, J.; Baonza, V. G. Raman spectroscopy of aqueous methanol solutions under pressure. *High Pressure Res.* **2006**, *26*, 407−410.
(53) Lin, K.; Hu, N. Y.; Zhou, X. G.; Liu, S. L.; Luo, Y. Reorientation dynamics in liquid alcohols from Raman spectroscopy. *J. Raman Spectrosc.* **2012**, *43*, 82−88.
(54) Onori, G.; Santucci, A. Dynamical and structural properties of water/alcohol mixtures. *J. Mol. Liq.* **1996**, *69*, 161.
(55) Keefe, C. D.; Gillis, E. A. L.; MacDonald, L. Improper hydrogen-bonding CH center dot Y interactions in binary methanol systems as studied by FTIR and Raman spectroscopy. *J. Phys. Chem. A* **2009**, *113*, 2544−2550.
(56) Shimoaka, T.; Katsumoto, Y. Blue shift of the isolated CD stretching band of CH2DOH in water induced by changes in the hydrogen-bonding pattern. *J. Phys. Chem. A* **2010**, *114*, 11971−11976.
(57) Yu, Y. Q.; Wang, Y. X.; Hu, N. Y.; Lin, K.; Zhou, X. G.; Liu, S. L. Overlapping spectral features and new assignment of 2-propanol in the C-H stretching region. *J. Raman Spectrosc.* **2014**, *45*, 259−265.
(58) Yu, Y. Q.; Wang, Y. X.; Hu, N. Y.; Lin, K.; Zhou, X. G.; Liu, S. L. C-beta-H stretching vibration as a new probe for conformation of n-propanol in gaseous and liquid states. *Phys. Chem. Chem. Phys.* **2016**, *18*, 10563−10572.
(59) Yu, Y. Q.; Wang, Y. X.; Lin, K.; Zhou, X. G.; Liu, S. L.; Sun, J. New spectral assignment of n-propanol in the C-H stretching region. *J. Raman Spectrosc.* **2016**, *47*, 1385−1393.
(60) Wang, Y. X.; Zhu, W. D.; Lin, K.; Yuan, L. F.; Zhou, X. G.; Liu, S. L. Ratiometric detection of Raman hydration shell spectra. *J. Raman Spectrosc.* **2016**, *47*, 1231−1238.
(61) Frisch, M. J.; Trucks, G. W.; Schlegel, H. B.; Scuseria, G. E.; Robb, M. A.; Cheeseman, J. R.; Scalmani, G.; Barone, V.; Mennucci, B.; Petersson, G. A.; et al. *Gaussian 09*, revision B.01; Gaussian, Inc.: Pittsburgh, PA, 2009.
(62) Boys, S. F.; Bernardi, F. Calculation of small molecular interactions by differences of separate total energies − some procedures with reduced errors. *Mol. Phys.* **1970**, *19*, 553−566.
(63) Yu, Y. Q.; Wang, Y. X.; Lin, K.; Hu, N. Y.; Zhou, X. G.; Liu, S. L. Complete Raman spectral assignment of methanol in the C-H stretching region. *J. Phys. Chem. A* **2013**, *117*, 4377−4384.
(64) Liu, S. L.; Fourkas, J. T. Orientational time correlation functions for vibrational sum-frequency generation. 3. methanol. *J. Phys. Chem. C* **2015**, *119*, 5542−5550.
(65) Ishiyama, T.; Sokolov, V. V.; Morita, A. Molecular dynamics simulation of liquid methanol. II. Unified assignment of infrared, raman, and sum frequency generation vibrational spectra in methyl C-H stretching region. *J. Chem. Phys.* **2011**, *134*, 024510.
(66) Merrick, J. P.; Moran, D.; Radom, L. An evaluation of harmonic vibrational frequency scale factors. *J. Phys. Chem. A* **2007**, *111*, 11683−11700.
(67) Arunan, E.; Desiraju, G. R.; Klein, R. A.; Sadlej, J.; Scheiner, S.; Alkorta, I.; Clary, D. C.; Crabtree, R. H.; Dannenberg, J. J.; Hobza, P.; Kjaergaard, H. G.; Legon, A. C.; Mennucci, B.; Nesbitt, D. J. Defining the hydrogen bond: An account (IUPAC Technical Report). *Pure Appl. Chem.* **2011**, *83*, 1619−1636.

DOI: 10.1021/acs.jpcb.7b06036
J. Phys. Chem. B 2017, 121, 8179−8187

(68) Bako, I.; Megyes, T.; Balint, S.; Grosz, T.; Chihaia, V. Water-methanol mixtures: topology of hydrogen bonded network. *Phys. Chem. Chem. Phys.* **2008**, *10*, 5004−5011.
(69) Li, Q. Z.; An, X. L.; Gong, B. A.; Chengf, J. B. Cooperativity between OH center dot center dot center dot O and CH center dot center dot center dot O hydrogen bonds involving dimethyl sulfoxide-H2O-H2O complex. *J. Phys. Chem. A* **2007**, *111*, 10166−10169.
(70) Li, Q. Z.; An, X. L.; Gong, B.; Cheng, J. B. Spectroscopic and theoretical evidence for the cooperativity between red-shift hydrogen bond and blue-shift hydrogen bond in DMSO aqueous solutions. *Spectrochim. Acta, Part A* **2008**, *69*, 211−215.

DOI: 10.1021/acs.jpcb.7b06036
J. Phys. Chem. B 2017, 121, 8179−8187